Building and Environment 83 (2015) 91–103

Contents lists available at ScienceDirect

Building and Environment

journal homepage: www.elsevier.com/locate/buildenv

Temporal and spatial variability of urban heat island and thermal comfort within the Rotterdam agglomeration

L.W.A. van Hove [a, b, *], C.M.J. Jacobs [c], B.G. Heusinkveld [a], J.A. Elbers [c], B.L. van Driel [a], A.A.M. Holtslag [a]

[a] Wageningen University, Meteorology and Air Quality Group, PO Box 47, 6700 AA Wageningen, The Netherlands
[b] Wageningen University, Earth System Science Group, PO Box 47, 6700 AA Wageningen, The Netherlands
[c] Wageningen UR, Alterra, Climate Change and Adaptive Land Management (CALM), PO Box 47, 6700 AA Wageningen, The Netherlands

ARTICLE INFO

Article history:
Received 15 June 2014
Received in revised form
20 August 2014
Accepted 27 August 2014
Available online 6 September 2014

Keywords:
Urban heat island
Outdoor thermal comfort
Physiologically equivalent temperature (PET)
Intra-urban variability
Land use fractions
Urban geometry

ABSTRACT

This paper reports on temporal and spatial variability of local climate and outdoor human thermal comfort within the Rotterdam agglomeration. We analyse three years of meteorological observations (2010–2012) from a monitoring network. Focus is on the atmospheric urban heat island (UHI); the difference in air temperature between urban areas and rural surroundings. In addition, we calculate the Physiologically Equivalent Temperature (PET) which is a measure of thermal comfort. Subsequently, we determine the dependency of intra-urban variability in local climate and PET on urban land-use and geometric characteristics. During a large part of the year, UHI-intensities in densely built areas can be considerable, under calm and clear (cloudless) weather conditions. The highest maximum UHI-values are found in summer, with 95-percentile values ranging from 4.3 K to more than 8 K, depending on the location. In winter, UHI-intensities are generally lower. Intra-urban variability in maximum UHI-intensity is considerable, indicating that local features have an important influence. It is found to be significantly related to building, impervious and green surface fractions, respectively, as well as to mean building height.

In summer, urban areas show a larger number of discomfort hours (PET > 23 °C) compared to the reference rural area. Our results indicate that this is mainly related to the much lower wind velocities in urban areas. Also intra-urban variability in thermal comfort during daytime appears to be mainly related to differences in wind velocity. After sunset, the UHI effect plays a more prominent role and hence thermal comfort is more related with urban characteristics.

© 2014 The Authors. Published by Elsevier Ltd. This is an open access article under the CC BY-NC-ND license (http://creativecommons.org/licenses/by-nc-nd/3.0/).

1. Introduction

In the coming decades, sustainable urban planning faces two major challenges: first, the impact of climate change and the necessity for adaptation measures to mitigate the consequences, and second, that of urbanization and the necessity of balancing the various conflicting spatial demands. Climate change projections suggest that European summer heat waves will become more frequent and severe during this century, consistent with the observed trend of the past decades [1]. This will also be true for northwest Europe, including the Netherlands [2]. While urban areas will generally be exposed to the same change in regional climate as the surrounding area, the urban setting can exacerbate the impact of this exposure on a local scale. In addition, urbanization will continue in the next decades. Future projections for the Netherlands show a large expansion of the urban landscape, particularly in the western and central parts, of up to 20% in the next decades [3,4]. Both developments may significantly influence future urban climate conditions, thermal comfort of citizens and liveability of urban areas. Recent results indicate that outdoor thermal comfort and heat stress will likely become a critical issue in many urban areas in the Netherlands [5].

The presence of many buildings and artificial surfaces at the expense of open ground, open water and vegetation creates unique local climates altering temperature, moisture, wind patterns, and radiation. Consequently, local climate may vary considerably within cities. To ensure an effective and coherent development of adaptation strategies aimed at improvement of the urban thermal environment, a better understanding of the spatial and temporal

* Corresponding author. Wageningen University, Meteorology and Air Quality Group/Earth System Science Group, PO Box 47, 6700 AA Wageningen, The Netherlands.
E-mail address: Bert.vanHove@wur.nl (L.W.A. van Hove).

http://dx.doi.org/10.1016/j.buildenv.2014.08.029
0360-1323/© 2014 The Authors. Published by Elsevier Ltd. This is an open access article under the CC BY-NC-ND license (http://creativecommons.org/licenses/by-nc-nd/3.0/).

variability in local climate (intra-urban variability), and the influence of urban features thereon is needed.

To date, relatively few long-term observational data on the spatial variability of local climate within cities are available [6]. The climatological description of a city is often based on one or a few fixed meteorological stations, usually located in the city centre, or at the airport, and therefore not representative of the whole city. Information about the spatial variability in local climate usually applies to a limited period of time (for example based on observations obtained in dedicated measuring campaigns).

A distinct feature of urban climate is the urban heat island (UHI). A distinction can be made between surface UHI, the difference in surface temperatures between the urban and rural area, and the atmospheric urban heat island, the corresponding differences in air temperature. Furthermore, two types of atmospheric UHI can be distinguished, that of the Urban Boundary Layer (UBL) and that of the Urban Canopy Layer (UCL) [6].

For outdoor thermal comfort the UCL-UHI is the most important one since people live in the urban canopy layer. Therefore, the UCL-UHI is the most commonly observed of the two atmospheric types and often the one referred to in discussions of urban heat islands. In contrast to the surface UHI, the atmospheric UHI is mainly a nocturnal phenomenon; it often weak during the late morning and throughout the day and becomes more pronounced after sunset due to the slow release of heat from urban infrastructure. So, maximum UHI intensities (UHI_{max}) are usually reached after sunset as a result of slower cooling down of the urban areas as compared to the rural surroundings [7].

Outdoor thermal comfort is often implicitly linked with the UHI phenomenon [6]. However, human thermal comfort not only depends on air temperature but on the combined effect of air temperature, wind speed, air humidity and radiation [8]. Recent results of Ketterer and Matzarakis [9] indicate that air temperature alone is not an appropriate measure to quantify the intra-urban spatial variability of climate with respect to human thermal comfort.

The impact of land cover buildings, impervious and green surfaces, on local air temperatures has been well documented (see Ref. [10] for a literature review). An increase of the built-up area at the expense of natural surfaces like vegetation, open ground or water causes a change in the surface energy balance resulting into higher surface and air temperatures. Conversely, heating of urban areas may be lowered by increasing the vegetation area [11–15]. Urban geometry relating to the height and spacing of buildings is considered to be another important feature determining local climate because of its effect on radiation and air flow. Important parameters are the surface albedo, mean building height, ratio between mean building height and mean street width (height-to-width ratio or aspect ratio), and the sky view factor (SVF) [16–18].

In many studies, the influence of one or a few of the aforementioned urban landscape parameters has been examined. However, only a limited number of studies have applied a more integrative assessment, taking all urban landscape parameters into account [11,15,19–21]. Consequently, the relative importance of the urban landscape parameters in affecting local climate is unclear.

This paper reports on the urban climate within the Rotterdam agglomeration, the second largest city in The Netherlands. Results from earlier meteorological observations indicate the existence of a considerable UHI in densely built areas with values reaching up to 8 K or more [22,23]. The municipality of Rotterdam wishes to anticipate on current and future challenges for human thermal comfort by mainstreaming adaptation measures in the reconstruction of older neighbourhoods and development of new urban areas. In this context, a monitoring network has been established in 2009 [24]. It currently consists of 14 fixed Automatic Weather Stations (AWS).

In our study, we analyse three years of meteorological observations (2010–2012). All meteorological variables relevant for thermal comfort (that is, air and globe temperature, humidity, wind speed, radiation) are monitored by the monitoring network. As such also an indication about the intra-urban variability in human thermal comfort can be obtained. We focus on the conditions in the UCL. For this layer, we evaluate the UHI and calculate the Physiologically Equivalent Temperature (PET). The latter is a sophisticated measure of thermal comfort based on the energy balance of the human body [8].

The study has been carried out in the framework of Climate Proof Cities (CPC) [25]. The main objectives are: 1) to assess the temporal and spatial variability of local climate and human thermal comfort, and 2) to quantify the dependency of this intra-urban variability on the various urban features.

The main research questions are: 1) how large is the intra-urban variability in local climate and that of outdoor thermal comfort, and to what extent are these two linked, 2) to what extent is this variability determined by local features, and 3) what is the relative importance of the urban landscape parameters in explaining local climate and thermal comfort?

The results of the study give important insight into the potential effectiveness of adaptation measures in city design aimed at mitigating the impact of climate change on the UHI and outdoor thermal comfort in urban areas in the Netherlands.

The paper is organised as follows. After a description of the material and methods (Section 2), we first discuss the intra-urban variability in local climate with a focus on UHI (Section 3.1). Next the intra-urban variability in outdoor thermal comfort for the summer months (June, July and August) is discussed (Section 3.2). We examine to what extent UHI and thermal comfort are connected. In Section 3.3, we discuss the dependence of intra-urban variability in UHI and that in thermal comfort on the various urban landscape parameters. This is done for the summer results; results obtained for the other seasons are presented in the Supplementary Material. Section 4 discusses remaining issues and areas for further research and Section 5 concludes the paper. Impressions of the areas surrounding the monitoring stations in the Rotterdam agglomeration are given in the Supplementary Material.

2. Material and methods

2.1. Study area

The Rotterdam agglomeration is located at the North Sea, at the mouth of the rivers Meuse and Rhine, in the Southwest of the Netherlands. The agglomeration is the industrial heart of the Netherlands and is home to one of the World's largest ports. It covers approximately 782,43 km^2 of land surface and has 1,175,477 inhabitants [26]. The city of Rotterdam itself has more than 600,000 inhabitants (2011 UN data) and covers 319 km^2. The municipality consists of 22 districts, which are again subdivided into 88 neighbourhoods. Most of the area lies several meters below sea level, and is situated on a sandy plain. The area, like the rest of the Netherlands, experiences a rather mild maritime climate with average minimum and maximum temperatures during winter of about 1 °C and 6 °C respectively, and average minimum and maximum temperatures during summer of about 12 °C and 22 °C respectively [27].

2.2. Monitoring network and data collection

The monitoring network became operational in August 2009 with 4 automatic weather stations (AWS) and was extended to a total of 14 AWS in 2010 (operational in June 2010). Thirteen of the

AWS are located in the urban area, covering a range of Urban Climate Zones (UCZ) [28] (Fig. 1). The monitoring results of these stations are compared with those of a reference AWS located in the rural area, north of Rotterdam.

The stations are standard Campbell Scientific weather stations equipped with a 4-component radiation sensor (Hukseflux NR01), shielded thermometer-hygrometer with radiation screen (model CS215L and model MET20, Campell Scientific, USA), radiation error of up to 0.75 K at wind speeds <1 m s^{-1}, with temperature accuracy of 0.4 K and relative humidity accuracy of 2% (range: 10–90% and 4% outside this range), a 0.15 m diameter black-bulb thermometer (Sensor Data, The Netherlands), and an ultrasonic 2D anemometer (Gill Windsonic, Gill Instruments, UK, accuracy 0.5 m s^{-1}). The AWS has a 2 m mast with a measuring height of 1.5 for temperature, humidity, black globe temperature and radiation, and a height of 2 m for wind speed and direction.

Table 1 lists the location characteristics of the monitoring stations. For an impression of the area surrounding each monitoring station the reader is referred to the Supplementary Material. The station Bolnes is located in an urban garden, the stations Hoogvliet and South in street canyons, the station Ridderkerk in an urban park, and the station Vlaardingen in a park setting, at a distance of about 36 m from a neighbourhood in the south. The stations Bernisse, Capelle, Lansingerland and Ommoord are situated on similar flat bitumen roofs in neighbourhoods (measuring height 5–6 m), the station Spaansepolder is situated on a flat bitumen roof in a business area (measuring height ~6 m), the station Centre on an overhanging bitumen roof in a street canyon (measuring height ~6 m), and the station Rijnhaven is situated on a pier in the harbour (measuring height ~4 m), at distance of about 60 m to the nearest building.

In addition, we utilize data obtained from the WMO station (WMO code 06344), operated by the Royal Netherlands Meteorological Institute (KNMI). It is located nearby the Rotterdam-The Hague airport, at a distance of about 700 m from the nearest buildings, on a clay ground at 4.8 m below sea level. The datasets from this station contain information on air temperature (0.1 m and 1.5 m) (accuracy 0.2 K), dew point temperature (accuracy 0.2 K), sunshine, global radiation, precipitation, cloud cover, visibility, barometric pressure, wind speed and direction. For technical specifications, the reader is referred to [27].

The data provided by the AWS are stored as half-hourly block averages, while those obtained from the KNMI station are hourly average data. Only complete datasets (that is, when all stations are operating simultaneously and produce reliable results) were analysed. Small data gaps of up to 2 h were filled by linear interpolation. Since the observations of the roof stations might not follow the concept of the urban canyon layer completely, they have been analysed separately.

The UHI data were corrected for the passage of weather fronts which may create a short-term high UHI response ('spike').

Climate maps for summer T_{min} and T_{max} show a temperature gradient (from the coastline moving inland) around Rotterdam of

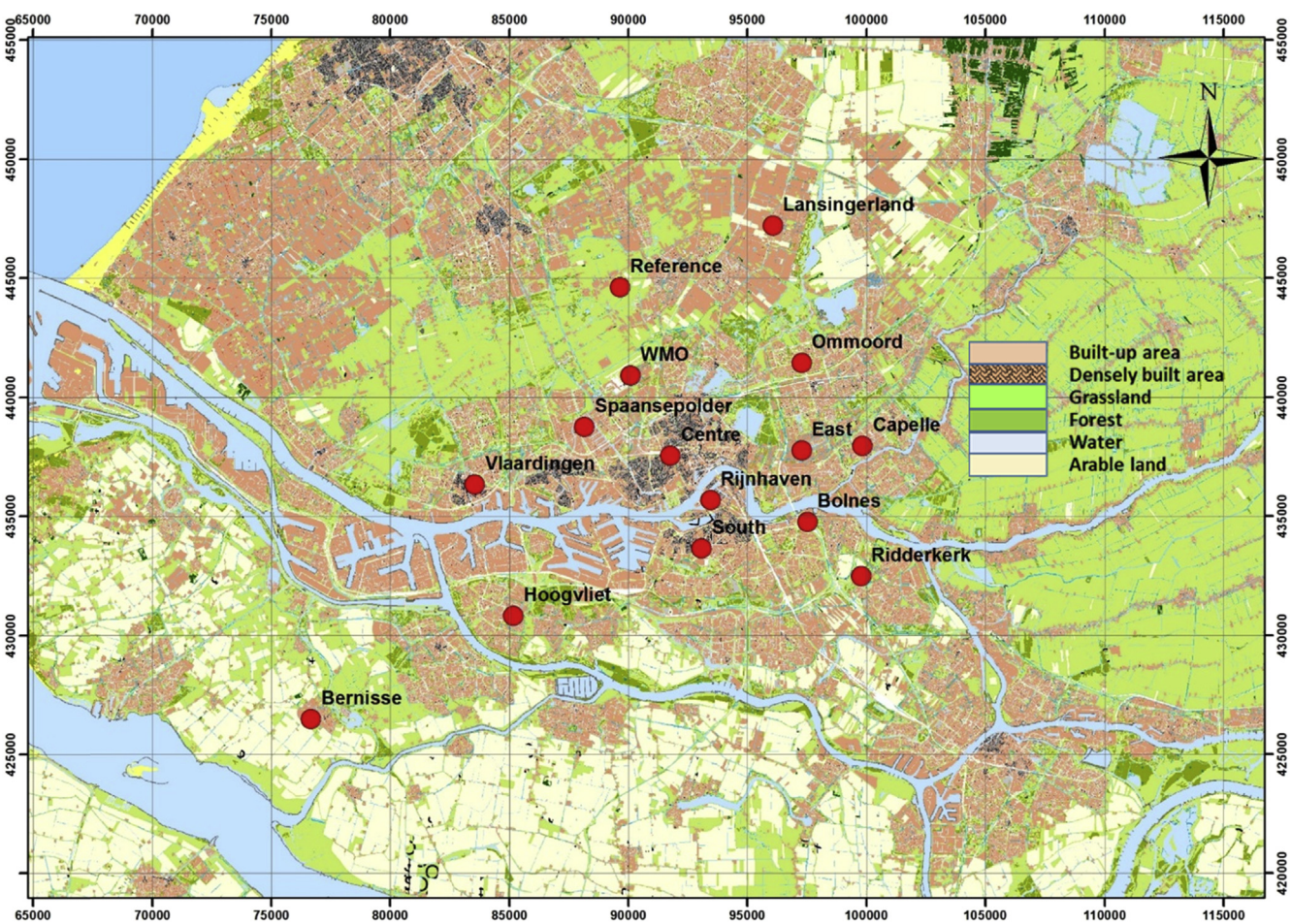

Fig. 1. Topographic map of the Rotterdam agglomeration and locations of the meteorological monitoring stations (see Table 1 for details and Supplementary Figure for impressions of the areas surrounding the stations). WMO station (WMO code 06344) is operated by the Royal Netherlands Meteorological Institute (KNMI). It is located nearby the Rotterdam-The Hague airport.

Table 1
Characteristics of the urban monitoring locations within the Rotterdam agglomeration.

	Name	Latitude	Longitude	Measuring height	Height ASL	% Building[a]	% Impervious	% Green	% Water	SVF	Element height	Surface albedo	Roughness[b] length (z_0)	Local climate zone[c]
Ground stations														
1	Bolnes	51.898	4.552	1.5	−1	10	39	25	2	0.60	2.54	0.08	0.03	CLR
2	Hoogvliet	51.861	4.374	1.5	0.5	16	38	32	9	0.63	6.41	0.08	0.28	CLR
3	Ridderkerk	51.878	4.585	1.5	−1	3	14	64	5	0.72	5.7	0.10	0.03	SB
4	South	51.887	4.488	1.5	2	39	71	4	0	0.53	10.34	0.06	0.85	CMR
5	Vlaardingen	51.911	4.349	1.5	−2	26	48	36	5	0.44	2.3	0.08	0.03	CLR
6	Airport (KNMI)	51.959	4.442	1.5	−7	4	12	86	2	0.98	0.03	0.13	0.03	Low Plants
7	Reference rural	51.986	4.436	1.5	−5	0	0	92	1	0.99	0	0.14	0.03	Low Plants
Roof stations														
8	Bernisse	51.821	4.251	6	−1	24	33	32	1	0.76	3.78	0.10	0.16	CLR
9	Capelle	51.927	4.585	5	−2	17	52	13	11	0.60	6.41	0.08	0.31	CLR
10	Centre	51.922	4.468	6	8	38	74	0	0	0.55	12.63	0.08	1.03	CHR
11	East	51.925	4.548	5	−3	11	23	20	25	0.68	6.12	0.07	0.26	OLR
12	Lansingerland	52.010	4.529	5	−5	27	40	17	4	0.56	3.9	0.08	0.17	CLR
13	Ommoord	51.958	4.547	5	−6	14	40	23	2	0.52	5.83	0.08	0.18	CLR
14	Spaansepolder	51.933	4.415	6	0	33	49	4	2	0.76	5.82	0.08	0.23	LLR
15	Rijnhaven[d]	51.906	4.493	4	0	18	40	4	39	0.78	26.61	0.06	2.62	OHR

[a] Land use fractions and geometric variables have been determined within a circular buffer area with a 250 m radius around a monitoring station.
[b] Calculated according to Grimmond and Oke [51].
[c] CLR compact low rise; CHR compact high rise; OLR open low rise; CMR compact median rise; LLR large low rise; SB sparsely built; OHR open high rise [28].
[d] Station 'Rijnhaven' is located on a 4 m high pier in the harbour, partially surrounded by high rise buildings (between 225° and 135°, distance to the nearest buildings 60–100 m.

about −0.014 K km^{-1} and 0.030 K km^{-1} respectively [27]. This gradient may influence our UHI statistics because the distance towards the coastline ranges from 18 to 32 km. The UHI signal was not corrected for this since it is unknown what the climate background gradient looks like in urban areas.

2.3. Calculation of the physiological equivalent temperature (PET)

The impact on human thermal comfort has been determined for the summer months June, July and August (JJA).

Hourly-average PET values were calculated with the RayMan model (version 1.2) using the default settings [29]: that is, a typical healthy male aged 35 years, weighing 75 kg, with a length of 1.75 m, standing outside, wearing moderate clothing (0.14 K m^2 W^{-1}) and doing light work (80 W). The measured globe temperature was used as an approximation of the mean radiant temperature (T_{mrt}) [30] that subsequently is an input parameter in the RayMan model. Thorsson et al. [30] report an uncertainty in T_{mrt} of less than ±3.5 °C with this method. From our results we can roughly estimate that this uncertainty gives an uncertainty in PET of less than ±1 °C. The blackness of the black globe may degrade in time. To check this we calculated for each AWS the monthly-mean difference between globe and air temperatures at a global radiation of >400 W m^{-2} and wind velocity <1.5 m s^{-1}. The decline in monthly-mean difference was then determined using the first monitoring month as a reference. Averaged over all stations, we found a change of +1% (±4%) after one year, and a change of +2% (±8%) in the second year.

The calculated PET values were subsequently related to thermal perception and grade of physiological stress according to the classification of Matzarakis et al. [31].

The calculated PET values may be regarded as spatially averaged values for an urban area in our study. Owing to various microclimate effects, such as shadowing by trees and thermal radiation from buildings or changed wind patterns by buildings or other obstacles, there may be large daytime differences in PET at the very local scale, down to the spatial scale of individual buildings and trees [31].

A complicating factor in the analysis is the difference in monitoring height between the roof and ground locations. This is particularly true for the calculation of PET. For instance, we calculated that the wind velocities monitored by the roof stations are 20–30% higher than those at 2 m height at these locations (results not shown here). So, the PET values calculated from the monitoring results of the roof stations are underestimations of the actual PET at ground level at these locations. However, the error made appears to be relatively small; −4 to +6% of the number of 'discomfort hours' (PET > 23 °C). Also the measured globe temperatures by the roof stations may differ from those at 2 m height because of differences in radiation effects. Since globe temperatures have been used to estimate PET [30], this may be an additional error in the calculation of PET at the roof locations. Despite these uncertainties, we find that the overall results for PET of the roof stations are consistent with those of the ground stations indicating that the errors made are probably small. Therefore, and given the complexity of transforming data from roof level to 2 m height level, we decided to present the results of the roof and ground stations separately, without applying any corrections.

2.4. Site characteristics

2.4.1. Surface cover fractions

For interpretation of the observations, in particular to correlate UHI intensity and PET to urban spatial parameters, it is important to know the footprint area or source area of a sensor. However, the conventional analytical footprint models have been developed for homogeneous and flat terrains [32]. Therefore, they are in principle unsuitable for application in the complex topography and heterogeneous terrain of urban areas. A more appropriate way to determine the footprints is probably by using advanced airflow models (see also [33]) but such models are still under development. The area of influence can also be found by an iterative procedure in which the footprint area is gradually increased to find the optimal correlation between land use and UHI [20,21,23]. In this study, we applied the latter method and assessed the surface cover fractions of the building, impervious, green and open water surface for circular buffer areas with a radius of 125, 250, 500, 750 and 1000 m, respectively, around the monitoring sites. The fraction of impervious surface represents the built environment, incorporating roads, parking lots, paved areas, buildings and roof tops. This type of surfaces typically has low albedo values and does not evaporate water unless some water is stored on them. The surface cover

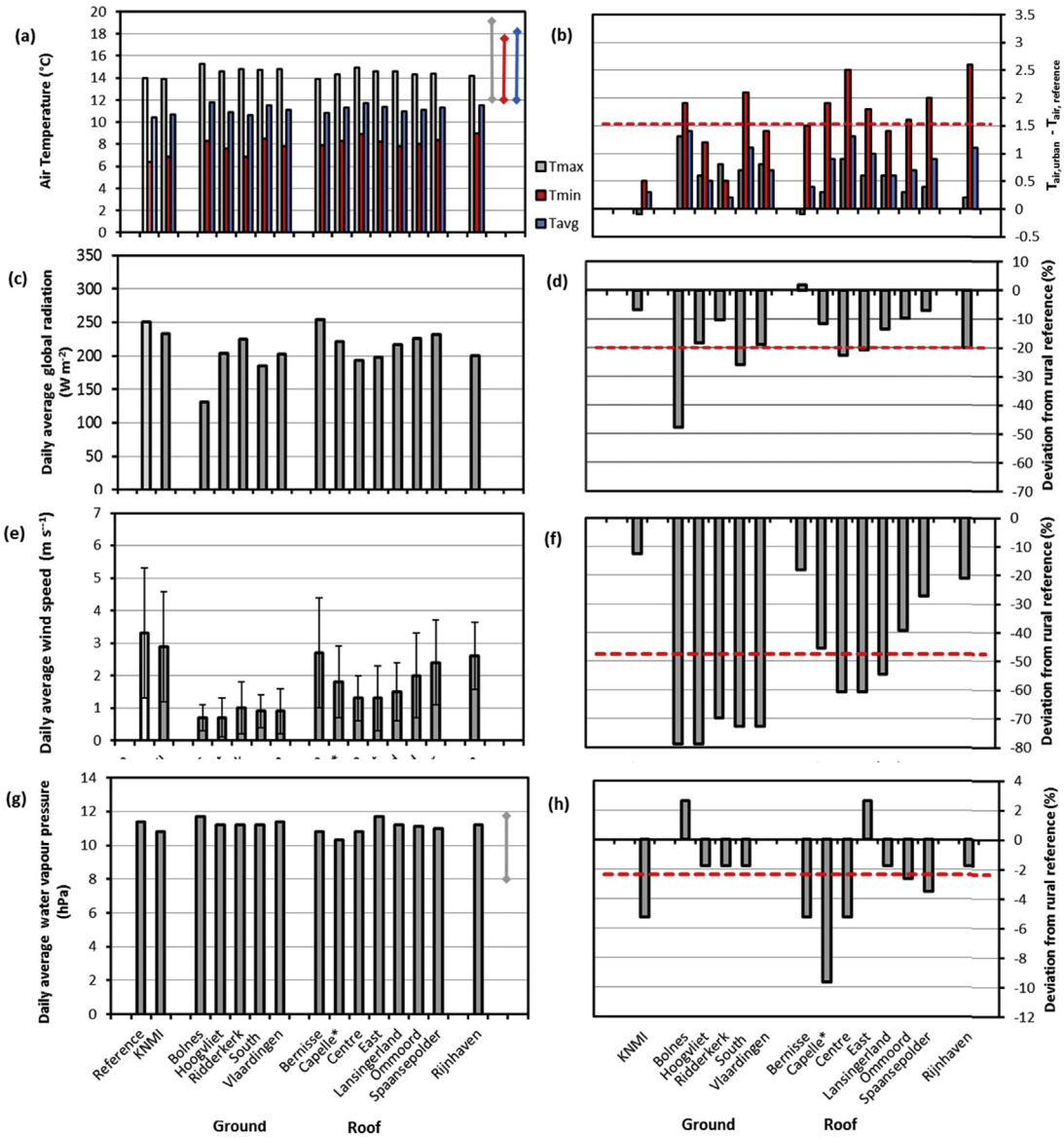

Fig. 2. Minimum and maximum air temperatures per day, daily-average air temperature (a), daily average global radiation (c), daily average wind speed (e) and daily average water vapour pressure (g). Average values for the period 1 July 2010–1 August 2012 are presented, for the ground and roof stations in the Rotterdam monitoring network. Panel (b): differences in maximum, minimum and daily average temperatures between the urban locations and the rural reference. Panels (d), (f), (h): % deviation from rural reference of daily average global radiation, daily average wind speed, and daily average water vapour pressure, respectively. The coloured arrows in upper right corner of (a) represent average standard deviations of maximum, minimum, and daily-average air temperatures, respectively. The arrow in the upper right corner of (g) represents average standard deviation of water vapour pressure. Error bars in (e) represent standard deviations of the wind speed. Horizontal dashed lines in (b) represents the average difference in minimum temperature between urban locations and rural reference location, horizontal dashed lines in (d), (f), and (h) represent the average % of deviation. *: limited dataset.

fractions were assessed with ArcGis10.1 using the topographical map 'Top10 2012' [34]. In addition, we used the most recent version of the land use database of the Netherlands (LGN6). The LGN database is raster database with 25*25 m resolution, it is covering the entire Dutch territory including urban areas, and presents the land use in 39 classes. From 1986 onwards the database is frequently updated with a 3–5 years interval (Centre Geo-information, Wageningen-UR). It is based on a combination of geo-data and satellite images [35].

2.4.2. Geometric characteristics

The geometric characteristics were determined for circular buffers with a radius of 250 m around each monitoring site. Both strong and no significant relationships are found at this radius (see Section 3.3). Since further analysis would not result into better results, we did not determine the influence of other circular buffers. Urban geometry was specified with the sky view factor (SVF), which quantifies the visible sky at a certain location. It is a dimensionless parameter that ranges from zero (no sky visible) to unity (no horizon obstructions visible). The advantage over other geometric measures like the height to width ratio H/W is that it is easier to assess a spatial average value for a complex environment [36]. The Sky View Factor (SVF) has been computed for each site from a 0.5 m resolution DEM AHN-2 database [37] for the Rotterdam-agglomeration ('Rotterdam-Rijnmond'). The DEM has a precision of approximately 5 cm. The solar algorithm of the SAGA-GIS software program [38] in combination with ArcGIS10.1 were used for this analysis. The settings in SAGA were: maximum search radius, 200; method: sectors; number of sectors; 180.

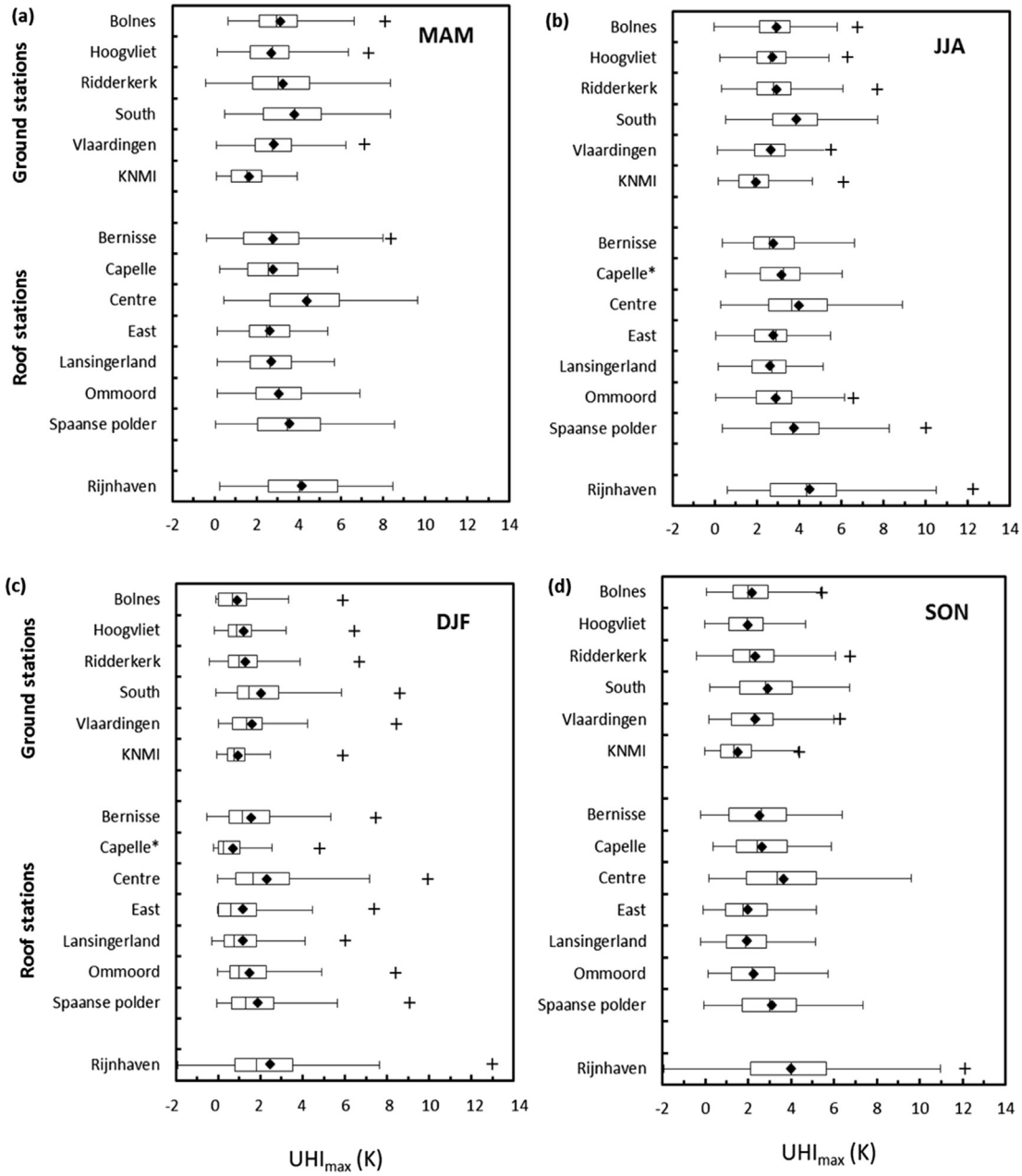

Fig. 3. Box whisker plots of UHI_{max} values in March, April and May (MAM) 2011, 2012) (a), in June, July and August (JJA) 2010–2012 (b), in December, January and February (DJF) 2010/2011, 2011/2012) (c), and in September, October and November (SON) 2010, 2011 (d). *: limited dataset; ◆ Average value, + Outlier.

The average height of all buildings and other obstacles like trees is known as the height of roughness elements. It was calculated by subtracting DEM data for surface level from DEM data including buildings, trees and other obstacles.

The average albedo value for each location was derived from cloud free Landsat images (resolution 30 by 30 m), which were acquired during the summer months June, July and August 2007 [39].

3. Results and discussion

3.1. Variation in local climate

An overview of the average meteorological conditions at the monitoring locations is given in Fig. 2. The average values have been calculated for the period July 2010–August 2012. All stations were simultaneously operational during more than 90% of the total number of hours in this period with the exception of AWS 'East' for which the gap fraction was 23%, and the AWS 'Capelle' that became operational in 2011. These rather complete sets of observations enabled reliable comparisons to be made. Note that, because of the data selection, the calculated values for the KNMI station may deviate from official statistics.

All urban locations show higher air temperatures as compared to the rural reference site or the KNMI station (Fig. 2(a and b)). The differences are larger for the minimum temperatures (0.5 K–2.6 K) than for the maximum temperatures (−0.1 K–1.3 K). This is not only true for the differences between urban stations and the rural reference site, but also for the mutual differences between the stations.

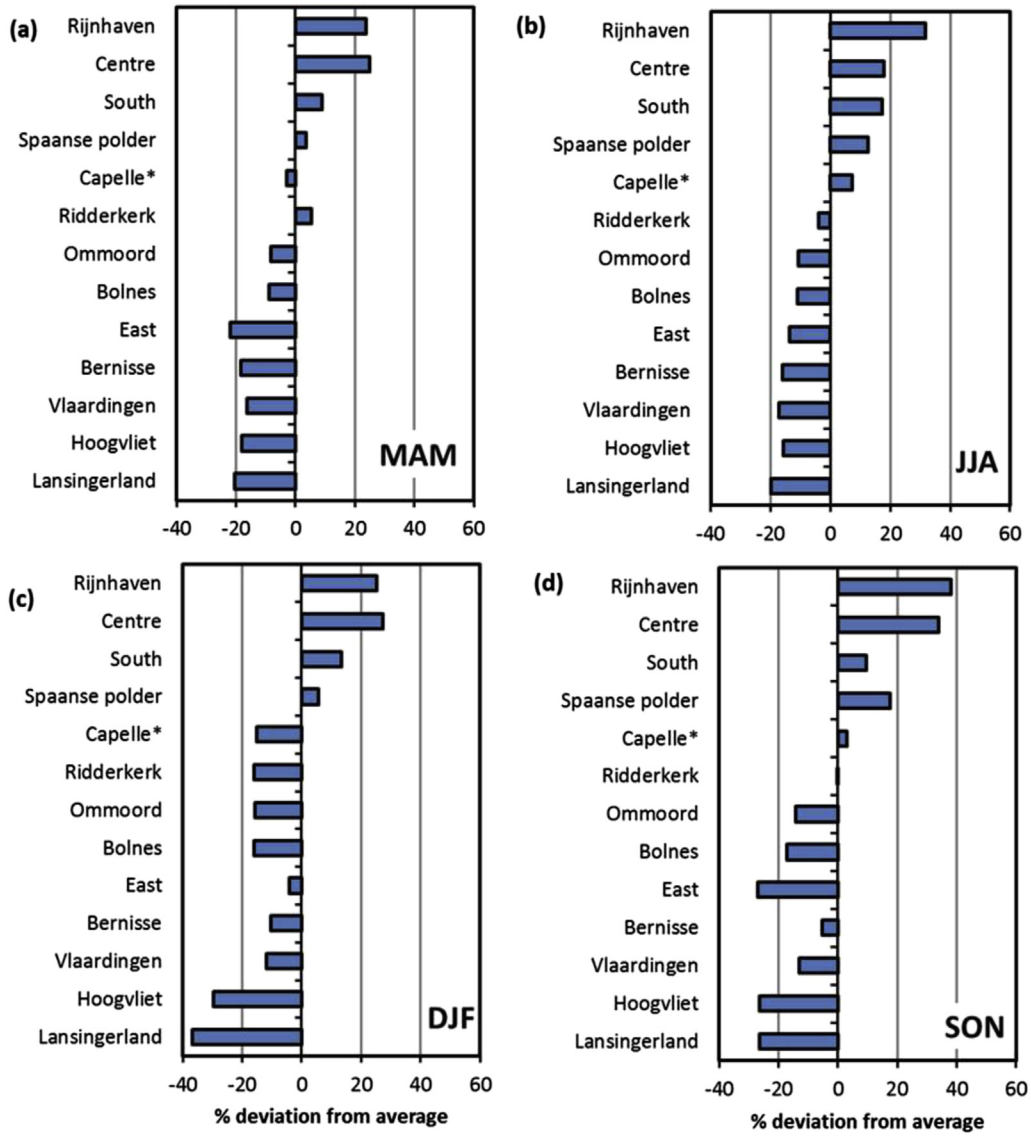

Fig. 4. Percentage deviation of average of UHI_{max} values in March, April and May (MAM) 2011, 2012 (a), in June, July and August (JJA) 2010–2012 (b), in December, January and February (DJF) 2010/2011, 2011/2012 (c), and in September, October and November (SON) 2010, 2011 (d). *: limited dataset.

During a large part of the year, UHI_{max} values in the built areas can be substantial (Fig. 3). High values are usually observed on clear (cloudless) days, with an easterly wind and low wind speed (<2 m s^{-1}) (that is, anticyclone flow). Only in winter time the UHI intensities are generally lower. However, even in this period UHI_{max} can reach 5 K or more. This appears to be mainly a short term effect (<1 day), often occurring when the wind direction changes to East or South-East and there is advection of cold air. While a fast cooling at the rural reference site occurs under these conditions, temperatures in the urban environment remain more or less constant. In late spring and summer the highest UHI_{max} values are found, with 95 percentile values varying from 4.3 K to more than 8 K depending on the location. In this period, the UHI intensity reaches its maximum already during the twilight hours (20:00–21:00 LT), remains at a constant maximum during a large part of the evening, and declines rapidly just before sunrise (5:00 LT).

In addition, we find substantial differences in UHI intensity within the agglomeration indicating that local urban characteristics have a strong influence on the UHI intensity. The mutual differences are larger in autumn and winter as compared to those of spring and summer (Fig. 4). Moreover, there is a seasonality influence on the ranking in magnitude of the UHI_{max} between the monitoring stations. In all seasons, however, the harbour location 'Rijnhaven', and the city locations 'Centre' and 'South' and the business area location 'Spaansepolder' show the highest UHI_{max} values.

With the exception of the roof station Bernisse, the urban stations show lower values (~16%) for the daily average global radiation as compared to the rural reference station (Fig. 2(c and d)). This can be attributed to shadowing effects of nearby buildings, trees or other obstacles. For instance, the sensor of 'Bolnes' is during the middle of the day in the shade of trees, which explains the low value found for this station. But lower values are also found for the roof stations 'Spaansepolder', 'Lansingerland', 'Ommoord' and the KNMI station of which the sensors are hardly influenced by nearby obstacles, suggesting that also a more polluted urban atmosphere causes the lower global radiation. However, on the other hand, the lower values measured by the urban stations may also be due to contamination of the sensors by the polluted urban air.

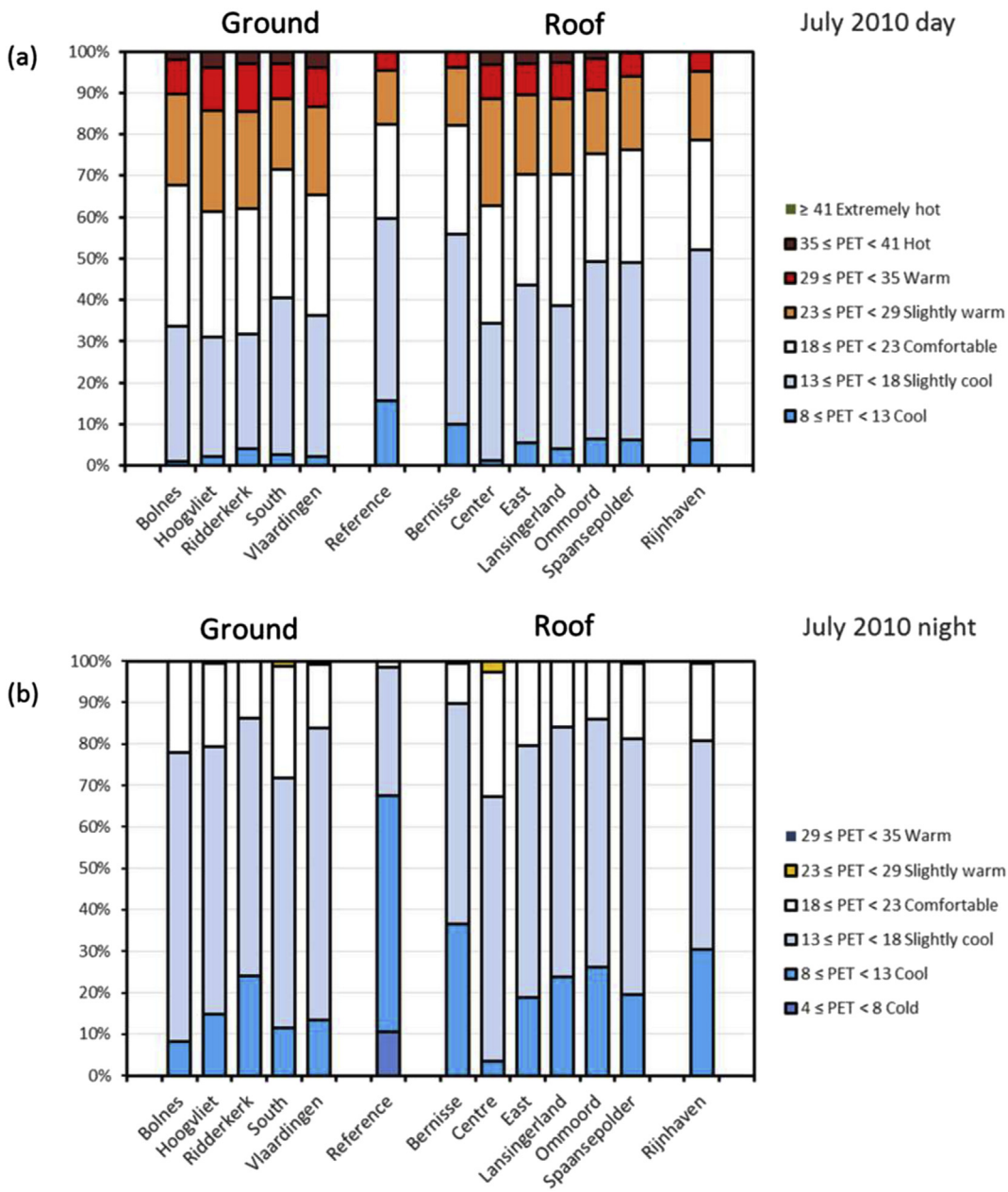

Fig. 5. Daytime 6:00–22:00 (LT) (a) and night-time (22:00–6:00) (b) frequency distributions of the different thermal comfort classes for July 2010.

Both roof and ground stations measure significantly lower wind speeds (44% and 65%, respectively) as compared to the reference rural site (Fig. 2(e and f)). The main wind directions at the reference station are from South-West to West (>33% of the total number of hours) which is also observed for most urban stations. Exceptions are the stations 'Bolnes' and 'South'. The former shows main wind directions between South and South-South-West, whereas no clear main wind direction is found for the urban station 'South' that is surrounded by high buildings on all sides (see also Supplementary Figure).

Minimum relative humidity at the urban locations is 9–15% lower (results not shown here) than in the rural reference area. This is largely due to the higher air temperatures since the daily average water vapour pressure in urban areas is only slightly lower (<2.3%) than in the rural area (Fig. 2(g and h)). The water vapour pressure in the rural site shows a diurnal variation, with higher values during daytime, whereas that in the urban area remains more or less constant. Similar results have been obtained by Kuttler et al. [40] for the city of Krefeld (Germany). The higher values in the rural area during daytime can be attributed to transpiration by the vegetation in the rural area.

3.2. Variation in local outdoor human thermal comfort

In the Netherlands, the highest air temperatures and global radiation are usually measured in July. Fig. 5 shows the frequency distributions for the different comfort classes for July 2010 at the 13 urban locations and at the rural reference location. The frequencies are expressed against the total number of daytime (6:00–22:00) and night-time hours respectively. All urban locations show a larger number of hours that can be classified as 'discomfort hours' (PET > 23 °C) as compared to the rural reference location. The

average number of discomfort hours at the urban locations during this month was ~157 h and ~93 h for the rural reference location (i.e. ~21.2% and ~12.5% respectively of the total number of hours). Exceeding of the PET 23 °C threshold value practically always occurred during the day. In 2011 and 2012, air temperatures in July were lower than the values averaged over 1981–2010 [27]). Although the average number of hours with PET>23 °C at the urban locations are less than in 2010 (32 h in 2011 and 77 h in 2012), relative differences between the locations are comparable to that of 2010.

In addition, Fig. 5 shows a substantial intra-urban variability in outdoor thermal comfort. This appears to be mainly related to the differences in wind velocity. We find a strong relationship between the frequencies of PET > 23 °C at the different locations and the average wind velocities in July 2010 (Fig. 6), explaining about 85% of the intra-urban variability. Comparable results have been obtained for the summer data of 2011 and 2012.

After sunset the UHI is more pronounced and consequently, night-time thermal comfort is likely to be more determined by this phenomenon. In order to get an impression how strong this dependency is, we determined the relationship between night-time thermal comfort and UHI intensity at the locations. This was not well possible for the 'discomfort hours' frequencies because exceeding of the PET 23 °C threshold value occasionally occurred during night-time in July 2010. The same is true for the cool summers of 2011 and 2012. Occurrence of a 'comfortable urban climate' (18°C < PET < 23 °C) at the urban locations was more common. Therefore, in Fig. 7, the frequencies of 'comfortable hours' have been plotted against the median UHI_{max} values in July 2010. A moderate to strong linear relationship is found explaining 60–70% of the intra-urban variability in number of occurrences of 'comfortable hours'. 'Outliers' are the locations 'Bernisse', 'Spaansepolder' and 'Rijnhaven' which are less comfortable than can be expected on basis of their UHI_{max} values. Also this may be related to the relatively high wind velocities at these locations.

3.3. Relation with local urban characteristics

The variety of urban environments represented by the 15 monitoring locations is illustrated by Fig. 8. It depicts the distribution of the land use classes within a buffer area with a radius of 250 m around each monitoring station.

We related the median and 95 percentile UHI_{max} values to land use descriptors and geometric variables by linear regression. Predictors for UHI_{max} were derived from linear relations with the highest r^2 (with a minimum of 0.30), and with slope p-values < 0.05.

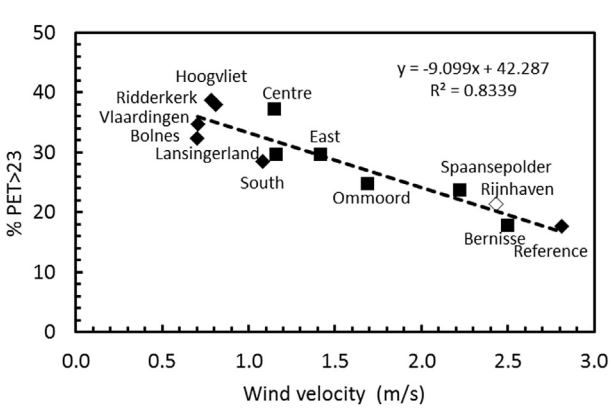

Fig. 6. Daytime 6:00–22:00 (LT) frequencies of PET > 23 °C in July 2010 at the 14 locations plotted against average daytime wind speeds in July 2010. ◆ ground stations; ■ roof stations; ◇ harbour station 'Rijnhaven'.

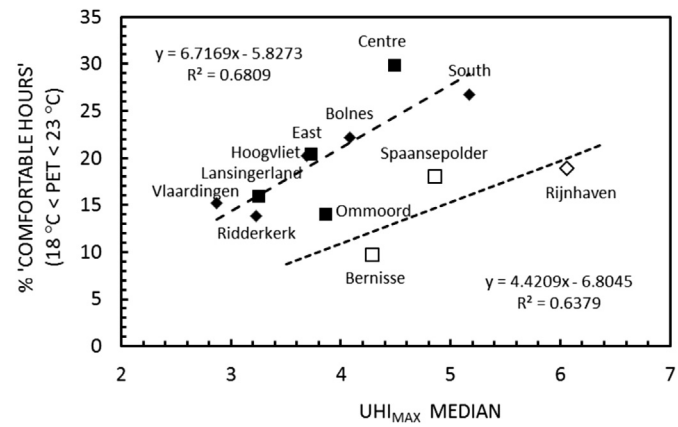

Fig. 7. Night-time frequencies of 'comfortable hours (18°C < PET < 23 °C) in July 2010 at the 14 locations plotted against median UHI_{max} values in July 2010. ◆ ground stations; ■ roof stations; □ roof stations, wind velocity >1 m s^{-1}; ◇ harbour station 'Rijnhaven'.

The results of the correlation statistics for the months June, July and August (JJA) are presented in Table 2. For the building surface fraction, the optimal source area radius is 250 m for all stations. However, the roof stations show the highest r^2 values (and lowest p-values) for the linear relationships assessed for the 750 m radius, while for the ground stations the highest r^2 values are obtained for the 500 and 250 m radii. With one exception, similar optimal source area radii have been assessed for the impervious surface fraction. For the green surface fraction, the best relationships are found for the 250 m radius (roof stations) and 500 m radius (ground stations and ground plus roof stations).

Fig. 9 shows the obtained relationships between the median and 95 percentile UHI_{max} values for JJA (2010–2012) and the land surface fractions as well as the SVF and mean building height. The regression coefficients of all assessed relationships are given in Table 3 (see Supplementary Material for the other seasons).

The building surface fraction appears to be a moderate to strong predictor of UHI_{max} explaining about 50–90% of the intra-urban variability. Our results for all stations (Roof + Ground in Table 3) show that an increase in the building surface fraction of 0.1 (10%) will lead to an increase in the median and 95 percentile UHI_{max} values of 0.36 K and 0.63 K, respectively. The influence of the impervious surface fraction is less. When the fraction increases with 0.1, the median and 95 percentile UHI_{max} values increase with 0.22 K and 0.44 K, respectively. Similar regression coefficients are obtained for the relationships assessed for the median and 95 percentile UHI_{max} values in spring and autumn (2011,2012) (see Supplementary Material).

The dependency of UHI_{max} on the green surface fraction was only determined for the summer when the vegetation is active. We find that the green surface fraction is also a moderate to strong predictor of UHI_{max}, explaining 50–60% of the intra-urban variability. The median and 95 percentile UHI_{max} values decline with 0.33 K and 0.62 K, respectively, when the green surface fraction increases by 0.1. Overall our results do not show significant relationships between UHI_{max} and the open water surface fraction.

Also strong correlations ($r^2 = 0.69$–0.80 for all stations) for the influence of the average building height are found. When the average building height increases by 1 m, the median and 95-percentile values UHI_{max} values increase with 0.08 and 0.19 K respectively. In contrast, we find no significant relationships for SVF at a confidence level of 0.05. With one exception, the same is true for the surface albedo.

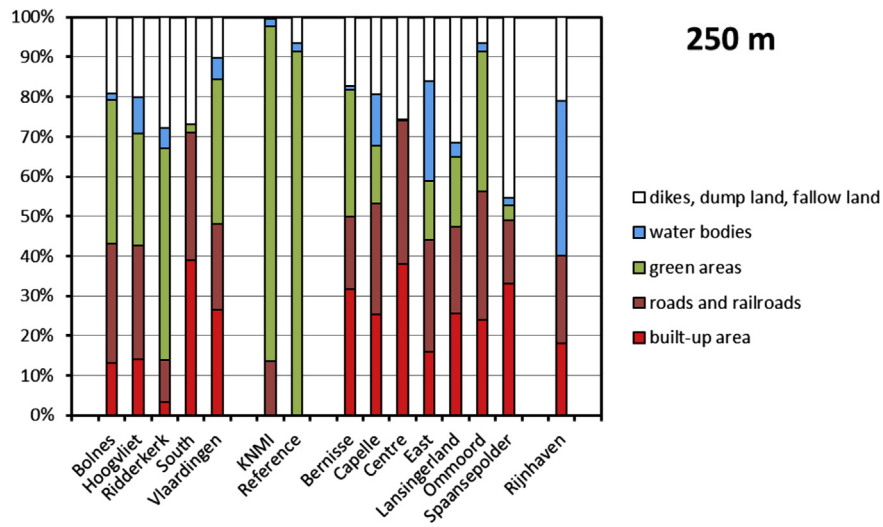

Fig. 8. Land use classes within a circular buffer area with a radius of 250 m around each monitoring location.

We also assessed the influence of urban characteristics on the number of occurrences of thermal discomfort (PET > 23 °C) for the summers of 2010–2012. As expected, because of the dominant influence of wind velocity on PET during the day, no significant relationships are found. Like discussed before, PET after sunset is determined more by the UHI (see Fig. 9). Hence, PET during nighttime is also significantly related to the urban features that show a significant relationship with UHI_{max}. This has indeed been found (results not shown here).

4. Discussion

Despite the presence of the North Sea and other large water bodies, UHI intensities at the different locations within the Rotterdam agglomeration can be substantial, under favourable meteorological conditions (i.e. under calm and clear weather conditions). Our results show that this is true for a large part of the year; only in winter, UHI-intensities are generally lower. The highest maximum UHI values are found in late spring and summer, with 95 percentile values ranging from 4.3 K to more than 8 K, depending on the location. These values are consistent with earlier observations in Rotterdam [22,23], and of the same order of magnitude as those reported for other European cities [41]. In addition, we find a substantial intra-urban variability in UHI intensity, indicating that local characteristics of the built environment have an important influence. It is interesting that also a UHI effect is found for the KNMI station at the airport. This can be explained by the plume effect of the built environment (see also Ref. [23]).

The present study provides quantitative information on the effects of land use and geometric features that support a more effective adaptation planning. We find a positive linear

Table 2
Correlation statistics for the median and 95 percentile UHI_{max} values in June, July, August (JJA) 2010–2012 and urban characteristics.

Urban land use	R^2 (p-value)						
	Radius (m)	Roof		Ground		Roof + ground	
		Median	P95	Median	P95	Median	P95
Building surface fraction	125	0.35 (0.16)	0.66 (0.03)	0.50 (0.12)	0.26 (0.31)	0.45 (0.01)	0.51 (<0.01)
	250	0.45 (0.10)	0.57 (0.05)	0.66 (0.05)	0.53 (0.10)	0.64 (<0.01)	0.54 (<0.01)
	500	0.56 (0.05)	0.74 (0.01)	0.70 (0.04)	0.49 (0.12)	0.56 (<0.01)	0.42 (0.02)
	750	0.75 (0.01)	0.87 (<0.01)	0.52 (0.11)	0.26 (0.31)	0.61 (<0.01)	0.54 (<0.01)
	1000	0.30 (0.20)	0.38 (0.14)	0.56 (0.09)	0.32 (0.24)	0.45 (0.01)	0.38 (0.02)
Impervious surface fraction	125	0.51 (0.07)	0.73 (0.01)	0.44 (0.15)	0.25 (0.31)	0.45 (0.01)	0.48 (<0.01)
	250	0.46 (0.10)	0.80 (<0.01)	0.69 (0.04)	0.48 (0.13)	0.58 (<0.01)	0.60 (<0.01)
	500	0.52 (0.07)	0.73 (0.01)	0.57 (0.08)	0.33 (0.24)	0.48 (<0.01)	0.52 (<0.01)
	750	0.67 (0.02)	0.81 (<0.01)	0.45 (0.14)	0.23 (0.34)	0.48 (<0.01)	0.50 (<0.01)
	1000	0.45 (0.10)	0.55 (0.06)	0.48 (0.13)	0.26 (0.30)	0.42 (0.02)	0.43 (0.01)
Green surface fraction	125	0.43 (0.11)	0.25 (0.25)	0.53 (0.06)	0.43 (0.11)	0.46 (0.01)	0.28 (0.06)
	250	0.85 (<0.01)	0.64 (0.03)	0.75 (0.01)	0.55 (0.06)	0.68 (<0.01)	0.42 (0.01)
	500	0.60 (0.04)	0.37 (0.15)	0.76 (0.01)	0.68 (0.02)	0.65 (<0.01)	0.48 (<0.01)
	750	0.70 (0.35)	0.26 (0.24)	0.72 (0.02)	0.55 (0.06)	0.45 (0.02)	0.27 (0.07)
	1000	0.08 (0.54)	0.23 (0.28)	0.70 (0.02)	0.54 (0.06)	0.40 (0.02)	0.27 (0.07)
Water surface fraction	No significant correlations (r^2 < 0.15)						
Urban geometry							
SVF	250	~0	~0	0.52 (0.10)	0.31 (0.25)	0.22 (0.11)	0.07 (0.38)
Mean building height	250	0.50 (0.07)	0.71 (0.02)	0.79 (<0.01)	0.91 (<0.01)	0.69 (<0.01)	0.80 (<0.01)
Surface albedo	250	0.15 (0.39)	0.11 (0.47)	0.74 (0.01)	0.52 (0.10)	0.30 (0.06)	0.08 (0.38)

The highest r^2 and lowest p values are shaded.

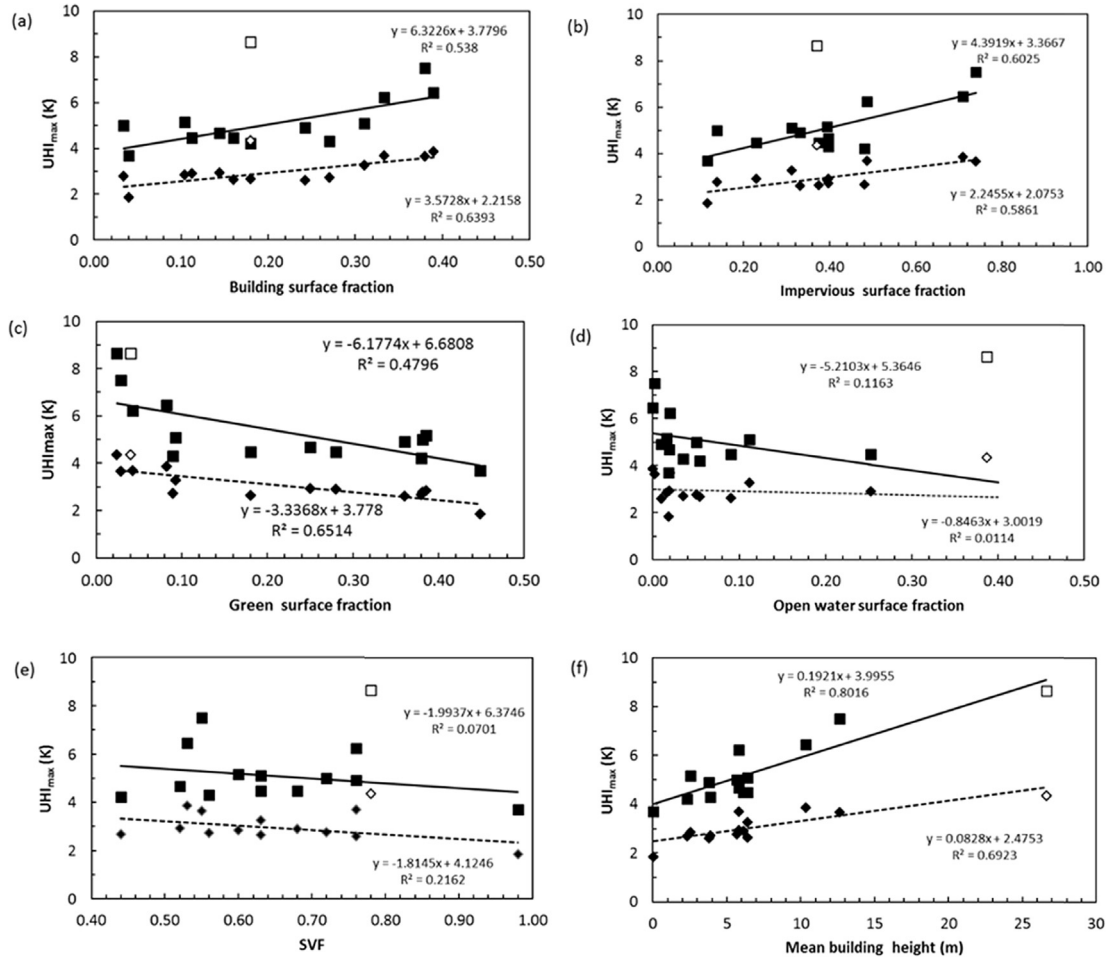

Fig. 9. Median and 95 percentile UHI_{max} values in June, July and August (JJA) 2010–2012 versus building surface fraction (a), impervious surface fraction (b), green surface fraction (c), open water surface fraction (d), Sky View Factor (SVF) (e), and mean building height (f). ◆ Median UHI_{max}; ■ 95 percentile UHI_{max}; ◇ Median UHI_{max} harbour station 'Rijnhaven'; □ 95 percentile UHI_{max} harbour station 'Rijnhaven'.

relationships between UHI_{max} and the building and impervious surface fraction and a negative linear relationship for the green surface fraction. These results are in accordance with those found in previous studies [11,15]. We find that most source area radii or foot print areas of these land cover fractions ranges between 250 and 500 m. These source area radii are of the same order of magnitude as found in other studies for air temperature measurements in cities with an urban morphology comparable to the one of Rotterdam [20,21,42], that is, mainly compact midrise buildings according to the UCZ classification of Stewart and Oke [28]. The source area radius may be much smaller for intensely developed urban areas. For instance, source area radii of 50 and 15–17 m have been reported for London and Hong Kong respectively [19,43].

Of the above land cover parameters, the building surface fraction appears to be strongest predictor of the intra-urban variability in UHI_{max}. Median and 95 percentile values of UHI_{max} in summer increase on average with 0.36 and 0.63 K respectively, when the fraction increases by 0.1. This is consistent with the efficient solar radiation absorption by the built-up area due to multiple reflection, and the large heat storage by buildings during the day: the stored heat is released again during night-time. Moreover, the released heat may be trapped between the buildings due to lack of ventilation [17].

In relatively 'green' urban areas, less overall heating of the urban area during the day occurs [44–46]. A part of the captured solar energy by the surface is used for evapotranspiration by the vegetation resulting into less warming of urban air and materials. Furthermore, less heating occurs due to shadowing effects of trees. So, green urban areas show less overall heat storage during the day and consequently a larger cooling down after sunset which explains the moderating influence of vegetation on nocturnal UHI [15].

The assessed regression coefficients for green surface fraction are comparable to those obtained with mobile traverse measurements in Rotterdam and data analysis of stations Centre, East, South, Rijnhaven and Airport over the same period [23], and to those reported for other cities and villages in the Netherlands [5]. Hence, the regression coefficient for the influence of the green surface fraction in an urban area appears to be a robust predictor of the intra-urban variability of UHI_{max}, at least for cities in the Netherlands.

An explorative model simulation study of Gill et al. [46] indicate that adding green in high-density residential areas and town centres offers a significant potential in moderating the increase in summer temperatures expected with climate change. The results of our study provide additional quantitative evidence for this.

The absence of a clear relationship between UHI_{max} and SVF seems to contradict the strong relationship ($r^2 = 0.88$) reported by Oke [17]. This relationship is, however, based on results obtained for urban areas belonging to the same UCZ, e.g. intensely developed, high density areas. Results of Svenson [47] demonstrate that in this case the strongest relationships between nocturnal air temperatures and SVF are obtained. More recent reported results

Table 3
Regression coefficients (±standard deviation) assessed from linear regressions between median or 95 percentile UHI_{max} values in JJA 2010–2012 and urban characteristics. For the land surface fractions, regression coefficients with the highest r^2 values and lowest p values are given (shaded values in Table 2).

Urban land use fractions	Range[a]	Roof		Ground		Roof + ground	
		Median	P95	Median	P95	Median	P95
Building	0.03–0.38	3.0 (±1.5)	8.9 (±3.4)	3.8 (±1.4)	5.3 (±2.7)	3.6 (±0.8)	6.3 (±1.5)
Impervious	0.14–0.74	2.1 (±0.7)	6.1 (±1.3)	2.4 (±0.8)	3.0 (±1.6)	2.2 (±0.6)	4.4 (±1.1)
Green	0.01–0.64	−3.7 (±0.8)	−8.4 (±2.7)	−4.3 (±0.6)	−8.2 (±1.6)	−3.3 (±0.6)	−6.2 (±1.8)
Water	0.00–0.39	ns	ns	ns	ns	ns	ns
Urban geometry							
SVF	0.44–0.78	ns	ns	ns	ns	ns	ns
Mean building height (m)	2.3–26.6	0.10 (±0.05)	0.33 (±0.09)	0.08 (±0.02)	0.18 (±0.02)	0.08 (±0.02)	0.19 (±0.03)
Surface Albedo	0.08–0.17	ns	ns	−27.3 (±7.2)	ns	ns	ns

[a] Without KNMI and Reference site; ns – no significant linear relationship at a confidence level of 0.05.

are less clear with respect to this relationship. Both strong, weak, and no significant relationships between SVF and UHI have been reported, even for the same urban areas (see Ref. [48] for review). According to Blankenstein and Kuttler [36] intra-urban variability in UHI cannot be predicted well with SVF alone, because it does not take spatially variable thermal properties of materials into account. Moreover, measured air temperature values can be affected by advection effects from the wider surroundings of a particular location.

The above landscape parameters appeared to have, however, a limited impact on the intra-urban variability in outdoor thermal comfort. During daytime the intra-urban variability is mainly determined by the differences in wind velocity between the locations. Differences in air humidity and global radiation in urban areas are relatively small and have no notable influence on the magnitude of PET. After sunset the UHI effect phenomenon is more pronounced and consequently, we find that outdoor thermal comfort is more related to the UHI effect and urban land scape parameters affecting this phenomenon.

Our results also indicate that a high UHI intensity at a location not always coincides with a large thermal discomfort. This is clearly demonstrated by the results of the harbour location 'Rijnhaven'. This location shows the highest UHI_{max} values. Owing to relatively high wind velocities, this location shows relatively low frequencies of 'discomfort hours' during the day on warm summer days. Moreover, frequencies of 'comfortable hours' during night-time are less than expected on basis of the UHI_{max} values.

The results of the harbour station 'Rijnhaven' also illustrate the complexity of the effect of open surface water on local climate in urban areas. The highest UHI_{max} values are found for all seasons suggesting that throughout the year, the river Maas has a night-time warming effect on the neighbouring urban area. However, in contrast, daytime air temperatures at this location are similar or sometimes even lower than those at the rural reference location. Consequently, the large water body may provide daytime cooling at this location on hot days in spring and summer. Moreover, it provides a free wind path (ventilation zone) and, as previously discussed, the higher wind speeds at this location directly reduce the PET. Results of Heusinkveld et al. [23] show that the daytime cooling effect diminishes during summer when the river water is warming up. This has also been observed by Hathway and Sharples [49] for a river in Sheffield, UK. Furthermore, their results demonstrate that the urban form on the river bank influences the levels of cooling felt away from the river bank. Thus, the ultimate effect of open surface water on local climate and thermal comfort strongly depends on season, time of the day, sizing (surface, depth) and the location with respect to upwind direction, and buildings and other structures in the surrounding area [50].

It can be concluded that one has to be cautious in applying the UHI effect as an indicator of outdoor thermal comfort. This would imply that heat island reduction programs may have a limited impact, and that also other summer cooling measures such as promoting natural ventilation in urban areas, have to be considered in order to improve outdoor human thermal comfort during hot summer days.

5. Conclusions

Our results show that during a large part of the year nocturnal UHI intensities in the densely built areas in the Rotterdam agglomeration can be considerable, in particular under calm and clear (cloudless) weather conditions. The highest maximum UHI values are found in late spring and summer, with 95 percentile values ranging from 4.3 K to more than 8 K, depending on the characteristics of the surrounding area of the monitoring station.

The present study provides quantitative information on the effects of land use and geometric features that support a more effective adaptation planning. Of all the urban features studied, we find that the intra-urban variability in UHI_{max} is significantly related to the building, impervious and green surface fractions, respectively, as well as to the mean building height. In particular, the building surface fraction appears to be a strong predictor for UHI_{max}, explaining 50–90% of intra-urban variability. Median and 95 percentile values of UHI_{max} in summer increase on average with 0.36 and 0.63 K respectively, when the fraction increases by 0.1. Similar results have been found for spring and autumn. The relationships obtained for the influence of the green surface fraction are consistent to those assessed in an earlier study for Rotterdam and for those assessed for other Dutch cities. Therefore, the green surface fraction in an urban area can be considered as a robust predictor of UHI_{max}, at least for cities in the Netherlands.

The above landscape parameters appeared to have, however, a limited impact on the intra-urban variability in outdoor thermal comfort. During daytime the intra-urban variability is mainly determined by the differences in wind velocity between the locations. Differences in air humidity and global radiation in urban areas are relatively small and have no notable influence on the magnitude of PET. After sunset the UHI effect phenomenon is more pronounced and consequently, we find that thermal comfort is more related to the UHI effect and urban land scape parameters affecting this phenomenon. Furthermore, our results indicate that UHI intensity at a location is not always a reliable indicator of outdoor thermal comfort.

Acknowledgement

The authors acknowledge the financial support from the Dutch Climate Changes Spatial Planning Programme, the Knowledge for Climate Research Programs, and the Municipality of Rotterdam. This study was also part of the strategic research program KBIV

'Sustainable spatial development of ecosystems, landscapes, seas and regions' which is funded by the Dutch Ministry of Economic Affairs, Agriculture and Innovation, and carried out by Wageningen University Research Centre(Project KB-14-002-005). We thank the Royal Netherlands Meteorological Institute for providing the observations from Rotterdam-Haaglanden airport, the Centre Geo-information of Wageningen UR for providing the necessary files for the ArcGIS analysis and for their technical support, and Waterwatch/e-leaf for providing the processed Landsat images. The authors cordially thank L. Gunst for providing pictures of the monitoring locations. We thank three anonymous reviewers for their useful comments that helped us to improve the manuscript.

Appendix A. Supplementary data

Supplementary data related to this article can be found at http://dx.doi.org/10.1016/j.buildenv.2014.08.029.

References

[1] Fischer EM, Schär C. Consistent geographical patterns of changes in high-impact European heat waves. Nat Geosci 2010:1–6.
[2] Van den Hurk B, Klein Tank A, Lenderink G, van Ulden A, van Oldenborgh GJ, Katsman C, et al. KNMI Climate Change Scenarios 2006 for the Netherlands, KNMI Scientific Report WR 2006-01. De Bilt: KNMI.
[3] Nijs T de, Crommentuijn L, Farjon H, Leneman H, Ligtvoet W, De Niet W, et al. Vier scenario's van het landgebruik in 2030. Achtergrondrapport bij de Nationale Natuurverkenning 2. RIVM rapport 408764003. Bilthoven: RIVM; 2002.
[4] MNP. Nationale Natuurverkenning 2, 2000–2030, Milieu- en Natuurplanbureau. Alphen aan de Rijn: Kluwer; 2002.
[5] Steeneveld GJ, Koopmans S, Heusinkveld BG, Van Hove LWA, Holtslag AAM. Quantifying urban heat island effects and human comfort for cities of variable size and urban morphology in the Netherlands. J Geophys. Res 2011;116:14. http://dx.doi.org/10.1029/2011JDO15988. D20129.
[6] Arnfield AJ. Two decades of urban climate research: a review of turbulence, exchanges of energy and water, and the urban heat island. Int J Climatol 2003;23:1–26.
[7] Oke TR. The energetic basis of the urban heat island. Q J R Met Soc 1982;108:1–24.
[8] Höppe P. The physiological equivalent temperature – a universal index for the biometeorological assessment of the thermal environment. Int J Biometeorol 1999;43:71–5.
[9] Ketterer Ch, Matzarakis A. Human-biometeorological assessment of the urban heat island in a city with complex topography – the case of Stuttgart, Germany. Urban Clim 2014. Available online, http://dx.doi.org/10.1016/j.uclim.2014.01.003.
[10] Chun B, Guldmann j-m. Spatial statistical analysis and simulation of the urban heat island in high-density central cities. Landsc Urban Plan 2014;125:76–88.
[11] Yokobori T, Ohta S. Effect of land cover on air temperatures involved in the development of an intra-urban heat island. Clim Res 2009;39(1):61–73.
[12] Ng E, Chen L, Wang Y, Yuan C. A study of the cooling effects of greening in a high-density city: an experience from Hong Kong. Build Environ 2012;47:256–71.
[13] Wong NH, Chen Y. Study of green areas and urban heat island in a tropical city. Habitat Int 2005;29(3):547–58.
[14] Bowler DE, Buyung-Ali L, Knight TM, Pullin AS. Urban greening to cool towns and cities; a systematic review of the empirical evidence. Landsc Urban Plan 2010;97(3):147–55.
[15] Yan H, Sh Fan, Ch Guo, Wu F, Zhang N, Dong L. Assessing the effects of landscape design parameters on intra-urban air temperature variability: the case of Beijing, China. Build Environ 2014;76. ISSN: 0360-1323:44–53.
[16] Bärring L, Mattsson J, Lindqvist S. Canyon geometry, street temperatures and urban heat island in Malmö, Sweden. J Climatol 1985;5(4):433–44.
[17] Oke T. Canyon geometry and the nocturnal urban heat island: comparison of scale model and field observations. J Climatol 1981;1(3):237–54.
[18] Eliasson I. Urban nocturnal temperatures, street geometry and land use. Atmos Environ 1996;30(3):379–92.
[19] Kolokotroni M, Giridharan R. Urban heat island intensity in London: an investigation of the impact of physical characteristics on changes in outdoor air temperature during summer. Sol Energy 2008;82:986–98.
[20] Houett T, Pigeon G. Mapping of urban climate zones and quantifying climate behaviors- an application on Toulouse urban area (France). Environ Pollut 2011;159:2180–92.
[21] Merbitz H, Buttstädt M, Michael S, Dott W, Schneider C. GIS-based identification of spatial variables enhancing heat and poor air quality in urban areas. Appl Geogr 2012;33:94–106. http://dx.doi.org/10.1016/j.apgeog.2011.06.008.
[22] Roodenburg J. Adaptation of rural minimum termperature forecasts to an urban environment. Arch Meteorol Geophys Bioclimatol 1983;32:395–401.
[23] Heusinkveld BG, Steeneveld GJ, van Hove LWA, Jacobs CMJ, Holtslag AAM. Spatial variability of the Rotterdam urban heat island as influenced by urban land use. J Geophys Res 2014;119:677–92. http://dx.doi.org/10.1002/2012JD019399.
[24] Van Hove LWA, Jacobs CMJ, Heusinkveld BG, Elbers JA, Steeneveld GJ, Koopmans S, et al. Exploring the urban heat island intensity of dutch cities. In: Hebbert M, Jankovic V, Webb B, editors. City weathers, meteorology and urban design 1950–2010. Manchester Architecture Research Centre, University of Manchester; 2011, ISBN 978-1-907120-98-5. http://www.sed.manchester.ac.uk/research/marc.
[25] Albers RAW, Bosch PR, Blocken B, Dobbelsteen AAJF, Van Hove LWA, Spit TJM, et al. Overview of challenges and achievements in the climate adaptation of cities and in the climate proof cities program. Build Environ 2014;82.
[26] Regionale Kerncijfers Nederland. Totale Bevolking Rotterdam (SG). The Hague, The Netherlands: Centraal Bureau voor de Statistiek; 2012.
[27] Royal Netherlands Meteorological Institute. Ministry of Infrastructure and Environment. www.knmi.nl/klimatologie. [accessed 02.04.14].
[28] Stewart ID, Oke TR. Local climate zones for urban temperature studies. Bull Am Meteorol Soc 2012;93(12):1879–900.
[29] Matzarakis A, Rutz F, Mayer H. Modelling radiation fluxes in simple and complex environments—application of the RayMan model. Int J Biometeorol 2007;51:323–34.
[30] Thorsson S, Lindberg F, Eliasson I, Holmer B. Different methods for estimating the mean radiant temperature in an outdoor urban setting. Int J Climatol 2007;27:1983–93.
[31] Matzarakis A, De Rocco M, Najjar G. Thermal bioclimate in Strasbourg – the 2003 heat wave. Theor Appl Climatol 2009;98. http://dx.doi.org/10.1007/s00704-009-0102-4.
[32] Schmid HP. Source areas for scalars and scalar fluxes. Boundary-Layer Meteorol 1993;67:293–318.
[33] Rannik U, Sogachev A, Foken Th, Gockede M, Kljun N, Leclerc MY, et al. Footprint analysis. In: Aubinet M, Vesala T, Papale D, editors. Eddy covariance. A practical guide to measurement and data analysis. Springer Science+-Business Media B.V; 2012, ISBN 978-94-007-2350-4. p.211–262. http://dx.doi.org/10.1007/978-94-007-2351-1. e-ISBN 978-94-007-2351-1.
[34] The Netherlands' Cadastre, Land Registry and mapping Agency. www.kadaster.nl/ [accessed 02.04.14].
[35] Hazeu GW, Schuiling C. New Dutch approach for land use mapping (LGN6). In: Proceedings of the third EARSeL workshop on land use and land cover, Bonn, Germany, 25–27 November, 2009. Bonn: EARSeL; 2009.
[36] Blankenstein S, Kuttler W. Impact of street geometry on downward longwave radiation and air temperature in an urban environment. Meteorol Z 2004;13(5):373–9.
[37] Publieke Dienstverlening op kaart (PDOK). https://www.pdok.nl/ [accessed 02.04.14].
[38] SAGA. System for automated geoscientific analyses. http://www.saga-gis.org/en/index.html [accessed 02.04.14].
[39] Waterwatch/e-Leaf. http://www.waterwatch.nl/. [accessed 02.04.14].
[40] Kuttler W, Weber S, Schonnefeld Ch, Hesselschwerdt A. Urban/rural atmospheric water vapour pressure differences and urban moisture excess in Krefeld, Germany. Int J Climatol 2007;27:2005–15.
[41] Memon RA, Leung DYC, Liu C-H. An investigation of urban heat island intensity (UHII) as an indicator of urban heating. Atmos Res 2009;94:491–500.
[42] Brandsma T, Wolters D. Measurement and statistical modeling of the urban heat island of the city of Utrecht (the Netherlands). J Appl Meteor Climatol 2012;51. http://dx.doi.org/10.1175/JAMC-D-11-0206.1.
[43] Giridharan R, Lau SSY, Ganesan S. Nocturnal heat island effect in urban residential developments of Hong Kong. Energy Build 2005;37:964–71.
[44] Gabor P, Jombach S. The relation between the biological activity and the land surface temperature in Budapest. Appl Ecol Environ Res 2009;7(3):241–51.
[45] Klok L, Zwart S, Verhagen H, Mauri E. The surface heat island of Rotterdam and its relationship with urban surface characteristics. Resour Conserv Recycl 2012;64:23–9. http://dx.doi.org/10.1016/j.resconrec.2012.01.009.
[46] Gill SE, Handley JF, Ennos AR, Pauleit S. Adapting cities for climate change: the role of the green infrastructure. Built Environ 2007;33(1):115–33.
[47] Svensson MK. Sky view factor analysis – implications for urban air temperature differences. Meteorol Appl 2004;11:201–11. http://dx.doi.org/10.1017/S1350482704001288.
[48] Unger J. Intra-urban relationship between surface geometry and urban heat island: review and new approach. Clim Res 2004;27:253–64.
[49] Hathway EA, Sharples S. The interaction of rivers and urban form in mitigating the urban heat island effect: a UK case study. Build Environ 2012;58:14–22.
[50] Theeuwes NE, Solcerová A, Steeneveld GJ. Modeling the influence of open water surfaces on the summertime temperature and thermal comfort in the city. J Geophys Res Atmos 2013;118:15. http://dx.doi.org/10.1002/jgrd.50704.
[51] Grimmond GSB, Oke TR. Aerodynamic properties of urban areas derived from analysis of surface form. J Appl Meteorol 1999;38:1262–92.